# Distinctive features of a continuous NMR in $^3$He-$B$, due to a spin supercurrent

A. S. Borovik-Romanov, Yu. M. Bun'kov, and V. V. Dmitriev, Yu. M. Mukharskiĭ,
E. V. Podd'yakova,[1)] and O. D. Timofeevskaya[2)]

*S. I. Vavilov Institute of Physics Problems, Academy of Sciences of the USSR, Moscow*
(Submitted 13 April 1989)
Zh. Eksp. Teor. Fiz. **96**, 956–972 (September 1989)

Experimental and numerical modeling was used to show that the behavior of the spin system of $^3$He-$B$ excited by a continuous-wave NMR is largely governed by the spatial transfer of the magnetization associated with gradients of the order parameter (superfluid spin current). These gradients form as a result of precession of the magnetization in an inhomogeneous magnetic field. It is shown that under certain conditions, a relatively weak rf field excites a homogeneously precessing domain in a chamber placed in an inhomogeneous magnetic field. The magnetization in this domain precesses in phase and is tilted by an angle close to 104° from the equilibrium orientation.

Investigations of the superfluid phases of $^3$He-$B$ by continuous-wave (cw) NMR methods are usually carried out employing a weak rf field. Under these conditions the NMR line of $^3$He-$B$ exhibits considerable inhomogeneous broadening because of the inhomogeneities of the magnetic field and of the order-parameter orientation (texture). The profile of this line is independent of the direction of scanning of the magnetic field. When the amplitude of the rf field is increased, the NMR line of $^3$He-$B$ loses its symmetry relative to the direction of scanning of the static field. Osheroff[1] and Webb[2] found that when a certain amplitude of the rf field was exceeded, the NMR absorption signal increased strongly when the NMR line was recorded in a decreasing static magnetic field. We shall show that this behavior of the NMR signal is due to the formation of a domain exhibiting spatially homogeneous precession of the magnetization (a homogeneously precessing domain or HPD). Formation of an HPD is due to two factors: firstly, the dipole–dipole shift of the precession frequency, which appears in $^3$He-$B$ at angles of tilt of the magnetization exceeding 104° (Ref. 3); secondly, the transfer of the magnetization by spin superfluid currents (supercurrents) due to order-parameter gradients induced by precession of the magnetization in an inhomogeneous magnetic field. This process is responsible for the formation of a region with a homogeneous precession of the magnetization where the angle of tilt of the magnetization from its equilibrium orientation is 104° and the inhomogeneity of the Larmor precession frequencies is compensated by a corresponding dipole–dipole frequency shift.

Such a homogeneously precessing region or an HPD was first observed in pulsed NMR experiments.[4,5] A theoretical explanation was given by Fomin.[6,7]

## 1. SPIN SUPERCURRENT AND NMR IN $^3$He-$B$

Since the Cooper pairing in superfluid $^3$He produces a state with a unique orbital and a spin moment, the order parameter has a more complex structure than in the case of $^4$He or in superconductors. It can be represented by a symmetric matrix (see, for example, the review in Ref. 8):

$$\hat{\psi}(\mathbf{k})=\begin{bmatrix}\psi_{\uparrow\uparrow} & \psi_{\uparrow\downarrow}\\ \psi_{\downarrow\uparrow} & \psi_{\downarrow\downarrow}\end{bmatrix}, \tag{1}$$

where $\mathbf{k}$ is a unit vector in the momentum space and governs the positions of Cooper pairs on the Fermi sphere of $^3$He-$B$. The three components of the order parameter can be regarded as order parameters of three superfluid components with the spin projections $-1$, 0, and 1 along a selected direction. It is usual to introduce the vector representation of the spin part of the order parameter:

$$\mathbf{d}(\mathbf{k})={}^1/_2 i(\sigma_y\sigma)_{\alpha\beta}\psi_{\alpha\beta}(\mathbf{k}), \tag{2}$$

where $\sigma$ are the Pauli matrices. The order parameter of $^3$He-$B$ can be described in terms of $\mathbf{k}$ as follows:

$$\mathbf{d}(\mathbf{k})=\Delta(T)e^{i\varphi}\hat{\mathbf{R}}(\mathbf{n},\theta)\mathbf{k},$$

where $\hat{\mathbf{R}}$ is the matrix of rotation about an axis $\mathbf{n}$ by an angle $\theta$; $e^{i\varphi}$ is a common phase factor. The order parameter can then be expressed in terms of the components of the vector $\mathbf{d}(\mathbf{k})$:

$$\psi=\begin{bmatrix}\psi_{\uparrow\uparrow} & \psi_{\uparrow\downarrow}\\ \psi_{\downarrow\uparrow} & \psi_{\downarrow\downarrow}\end{bmatrix}=\begin{bmatrix}-d_x(\mathbf{k})+id_y(\mathbf{k}) & d_z(\mathbf{k})\\ d_z(\mathbf{k}) & d_x(\mathbf{k})+id_y(\mathbf{k})\end{bmatrix}. \tag{3}$$

It is therefore clear that rotation of the vectors $\mathbf{d}$ about the $\mathbf{z}$ axis alters the phases of the wave functions $\psi_{\downarrow\downarrow}$ and $\psi_{\uparrow\uparrow}$ in such a way that if one rises, the second falls. If the vectors $\mathbf{d}(\mathbf{k})$ are inhomogeneous in the coordinate space, gradients of the phases of these functions appear, and they have opposite signs. This reverses the direction of the flow of the components $\psi_{\uparrow\uparrow}$ and $\psi_{\downarrow\downarrow}$ at a rate $v_{sp}=-\hbar\nabla\varphi/2m$, where $\nabla\varphi$ is the gradient of the phases of the components. The net transfer of mass by these fluxes is zero (if we ignore a small difference between the densities of the components $\psi_{\uparrow\uparrow}$ and $\psi_{\downarrow\downarrow}$, which appears in a magnetic field). On the other hand, the transfer of the magnetization by these fluxes is additive, which gives rise to a spin supercurrent.

The order parameter $\mathbf{d}(\mathbf{k})$ with gradients that determine the spin-current magnitude is not a physical quantity which can be measured directly. However, the motion of the magnetization $\mathbf{m}$ and of the vectors $\mathbf{d}(\mathbf{k})$ is related by the following equations of spin dynamics:

$$\begin{aligned}\dot{\mathbf{m}}&=\gamma[\mathbf{mH}]+\mathbf{R}_D,\\ \dot{\mathbf{d}}(\mathbf{k})&=\gamma[\mathbf{d}(\mathbf{k}),(\mathbf{H}-\chi^{-1}\mathbf{m})],\end{aligned} \tag{4}$$

where $\gamma$ is the gyromagnetic ratio for $^3$He, $\chi$ is the magnetic susceptibility of this substance, and $\mathbf{R}_D$ is the dipole moment.

The system of equations (4) is analogous to the systems

 0038-5646/89/090542-10$04.00  

of equations describing an antiferromagnetic resonance. Therefore, in the case of $^3$He-$B$ we can observe two NMR lines corresponding to precession of the magnetization (transverse mode) and oscillations of the magnitude of the magnetization (longitudinal mode). The dipole moment $\mathbf{R}_D$ depends on the orientation of the vectors $\mathbf{m}$ and $\mathbf{d}$. In the case of free precession of the magnetization the moment $\mathbf{R}_D$ vanishes for angles of tilt ($\beta$) of the magnetization up to arc cos($-1/4$) $\approx 104°$ and it rapidly rises for large tilt angles. Consequently, the frequency of the transverse NMR mode is equal to the Larmor value for tilt angles less than 104°. At higher tilt angles the NMR frequency is considerably higher than the Larmor frequency:

$$\omega = -\gamma H + \frac{16}{15}\frac{\Omega_B^2}{\gamma H}\left(\cos\beta - \frac{1}{4}\right), \tag{5}$$

where $\Omega_B$ is the frequency of the longitudinal mode and $\gamma$ is the gyromagnetic ratio (we recall that $\gamma < 0$ in the case of $^3$He).

Under NMR conditions both $\mathbf{m}$ and $\mathbf{d}(\mathbf{k})$ behave as a rigidly coupled system of vectors. The precession of the magnetization $\mathbf{m}$ corresponds to in-phase motion of the vectors $\mathbf{d}(\mathbf{k})$. The longitudinal NMR code corresponds to in-phase oscillations of $\mathbf{d}(\mathbf{k})$ in a plane perpendicular to $\mathbf{m}$. Consequently, spatial gradients of the order parameter are rigidly linked to gradients of the phase of precession (or longitudinal oscillations) of the NMR. In this way the gradients of the magnetization precession (oscillation) phases in $^3$He induce superfluid spin currents.

In describing the spatial magnetization transfer by a spin supercurrent we have to include also the gradient terms in Eq. (4). The general solution of the system becomes extremely cumbersome. However, Fomin[9] reduced the number of variables by using the characteristics of spin dynamics and the nature of the dipole potential of $^3$He-$B$ and thus obtained a system of equations describing the spatial dynamics of the magnetization in $^3$He-$B$ in the absence of an rf field. When all the gradients are directed along an external static magnetic field ($z$ axis), the system of equations is

$$\begin{aligned} &\frac{du}{dt} - \frac{1}{\omega}\frac{\gamma^2}{\chi}\frac{\partial}{\partial z}\left(\frac{\partial F_\nabla}{\partial \nabla\alpha}\right) = 0, \\ &\frac{d\alpha}{dt} + \omega - \frac{1}{\omega}\frac{\gamma^2}{\chi}\left(\frac{\partial F_\nabla}{\partial u} - \frac{\partial}{\partial z}\frac{\partial F_\nabla}{\partial \nabla u}\right) = 0. \end{aligned} \tag{6}$$

Here, $\alpha$ is the precession phase, $u = \cos\beta$ ($u > -1/4$), $\beta$ is the angle of tilt of the magnetization, and $F_\nabla$ is the gradient energy described by

$$\begin{aligned} F_\nabla = \frac{\chi}{\gamma^2}\Big\{ &(1-u)c^2(u)(\nabla\alpha)^2 \\ &+ \frac{1}{2}\frac{c^2(1)}{1-u^2}(\nabla u)^2 - \omega u(z-z_0)\gamma\nabla H \\ &+ \left[\frac{1}{2}\frac{3c^2(-1)}{(1+4u)(1+u)^2}u' \pm (1-u)\frac{c^2(-1)}{1+u}\left(\frac{3}{1+4u}\right)^{1/2}\nabla\alpha\right]\nabla u\Big\}, \end{aligned} \tag{7}$$

where $c^2(u) = uc_\parallel^2 + (1-u)c_\perp^2$; $c_\parallel$ and $c_\perp$ are the velocities of spin waves along and across the magnetic field, respectively. This expression for the gradient energy is obtained by minimization of the energy of the dipole–dipole interaction. It is assumed there that if $\beta > -1/4$, we have

$$\cos\beta + \cos\Phi + \cos\beta\cos\Phi = {}^1/_2, \tag{8}$$

which makes it possible to exclude the third phase of the order parameter $\Phi$ from the gradient energy. As $\cos\beta$ approaches $-1/4$, the value of $F_\nabla$ tends to infinity. This means that in a real system of $^3$He-$B$ the condition (8) is not satisfied in the vicinity of the point $\beta = 104°$ and, consequently, we have to minimize gradient and dipole energies simultaneously. If $\beta < -1/4$, minimization of the dipole energy leads to the condition $\Phi = 0$. Then, the expression for the gradient energy given by Eq. (7) should be modified by removing the term in square brackets.

The first equation in the system (6) is the law of conservation of the longitudinal magnetization. In other words, these equations ignore the processes of magnetic relaxation and, therefore, the validity of the solutions of this system of equations is limited to times shorter than the characteristic relaxation time. However, it has been found experimentally that there is a wide range of experimental conditions under which the processes of the magnetization transfer by a spin supercurrent in $^3$He-$B$ are much faster than the magnetic relaxation processes.[5] The first equation of the system (6) shows that the spin supercurrent transferring the longitudinal component of the magnetization is $\gamma\partial F_\nabla/\partial\nabla\alpha$. Using Eq. (7), we find that this spin supercurrent is described by:

$$\begin{aligned} J_{m_z} = -\frac{\chi}{\gamma}\Big\{ &2[(u-u^2)c_\parallel^2 + (1-u)^2c_\perp^2]\nabla\alpha \\ &\pm 3^{1/2}(2c_\perp^2 - c_\parallel^2)\frac{1-u}{1+u}(1+4u)^{-1/2}\nabla u\Big\}, \end{aligned} \tag{9}$$

provided $\cos\beta > -1/4$. The term with $\nabla u$ vanishes in the range where $\cos\beta < -1/4$. The system (6) is solved numerically in the Appendices 1 and 2. We shall show that the results of this numerical calculation are in good agreement with the experimental results.

## 2. EXPERIMENTS ON CONTINUOUS-WAVE NMR IN $^3$He-$B$

In the cw NMR method a sample experiencing a static magnetic field $\mathbf{H}_0$ is subjected to an rf field $\tilde{H}_1$ of small constant amplitude (pump field). If the rf field frequency becomes equal to the resonance frequency of the spin precession, the magnetic moment of a sample ($\mathbf{M}$) tilts away from its equilibrium orientation (along $\mathbf{H}_0$) and precesses in phase with $\tilde{H}_1$. An induction emf is then created in a receiving coil surrounding a sample and this emf is proportional to the magnetic moment $M_\perp$ which is at right-angles to $\mathbf{H}_0$. The receiving coil frequently performs also the function of creation of an rf field (receiving-transmitting coil).

A linearly polarized field $\tilde{H}_1$ can be expanded into two circularly polarized components and the value of each is $H_1 = \tilde{H}_1/2$. One of these components is polarized in the direction of precession of the magnetization. When speaking of the rf field, we shall imply specifically this component. The interaction of the magnetization with the other component varies rapidly with time (at twice the precession frequency) and averaging causes it to vanish.

We can distinguish two components of the precessing magnetic moment $\mathbf{M}_\perp$. One is the component $M_y$ perpendicular to $\mathbf{H}_1$ and the other is the component $M_x$ parallel to $\mathbf{H}_1$. The rf signal $I_y$, induced in the detection coil by the compo-

nent $M_y$, will be called absorption because the energy transferred to the system of nuclear magnetic moments in a sample by the rf field is proportional to $M_y$:

$$W=\omega M_y H_1=\omega M_\perp H_1 V \sin(\alpha-\varphi), \qquad (10)$$

where $\alpha$ is the phase of precession of the magnetic moment; $\varphi$ is the phase of the rf field; $V$ is the volume of the sample. The signal $I_x$ induced by the component $M_x$ is called dispersion. The absorption and dispersion signals are usually separated by a phase detection method that selects the component of the signal which is in phase with the reference signal and is rotated by an angle 90°. In our experiments the reference signal phase was selected using the characteristic dependence of the absorption and dispersion signals of the normal phase of $^3$He on the magnetic field. A correct tuning of the phase of the reference signal made the absorption signal into a function symmetric relative to the center of the NMR line and the dispersion signal an antisymmetric function.

We investigated experimentally cw NMR in $^3$He-$B$ at pressures of 0, 11, 20, and 29 bar using an rf field of frequencies 230, 460, and 780 kHz. We used different cells. The majority of the experiments were carried out in a chamber shown schematically in Fig. 1. A cell used for cw NMR, located in the upper part of the chamber, was a cylinder 6 mm in diameter and 6 mm long with its axis oriented along the external magnetic field. All internal surfaces of the cell were coated with a Mylar film. A receiving–transmitting rf coil created an rf field with a homogeneity of 10% across the size of the cell at right-angles to an external static field. A gradient of the static field was directed along the rf field and its magnitude could be measured within a wide range (from 0.01 to 25 Oe/cm). This cell was connected to the lower parts of the chamber where a sensor of a platinum NMR thermometer and a heat exchanger ensuring cooling of the helium were located: the connection was made by a channel 1 mm in diameter and 11 mm long. The chamber was placed on the nuclear step of a cryostat utilizing nuclear demagnetization of copper and constructed as described in Ref. 10.

The NMR signal of $^3$He was amplified with a wide-band amplifier. The absorption and dispersion signals were selected by a two-coordinate lock-in detector and recorded as well as processed with the aid of a computer. At low rf field amplitudes the profile and intensity of the NMR absorption and dispersion signals (representing the dependences of $I_x$ and $I_y$ on the magnetic field) were governed by the texture of the order parameter and by the inhomogeneity of the external magnetic field, but were independent of the field-scanning direction. However, when the rf field amplitude exceeded a certain threshold, the profile and amplitude of the NMR signals recorded during reduction of the field were greatly affected. The amplitude and the range of existence of these signals could increase by several orders of magnitude.

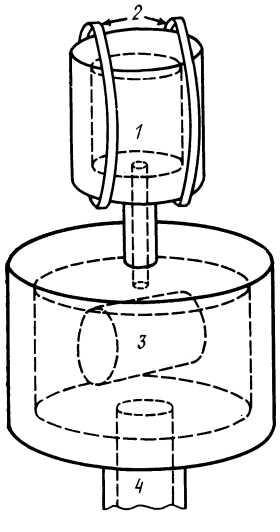


FIG. 1. Schematic diagram of the apparatus: 1) cell; 2) rf coils; 3) platinum NMR thermometer sensor; 4) channel leading to a chamber with a sintered silver heat exchanger.

Figure 2 shows typical absorption and dispersion signals obtained using a sufficiently high rf field and different directions of scanning by the external magnetic field when the field gradient was $\nabla H = 0.83$ Oe/cm. The following sections of the absorption signal recorded by reducing the field could be distinguished (Fig. 2a): a steep rise of the signal intensity in a narrow range of fields in the region of $H_a$, a continuous rise of the intensity from $H_a$ to $H_b$, a steep fall of the intensity in the region of $H_b$, a subsequent accelerated rise of the intensity, a jump of the intensity at $H_c$, and disappearance of the signal at $H_d$. If in any field from $H_a$ to $H_d$ the direction of scanning of the field was altered, the field dependence of the signal was retained everywhere with the exception of the region $H_c - H_{c'}$, where a hysteresis of the jump of the signal intensity was observed. If after disappearance of the signal the field was increased at $H_d$, it was found that the absorption signal intensity was much less in amplitude and the signal was detectable on this scale only near $H_a$. The field dependence of the intensity of the dispersion scale behaved similarly (Fig. 2b). The difference between the characteristic fields $H_a$ and $H_b$ was approximately equal to the difference between the maximum and minimum of the magnetic field across the size of the chamber. It rose linearly on increase in the magnetic field gradient. The absorption signals presented in Fig. 3 were obtained for different magnetic field gradients. The dependence of $H_a - H_b$ on the gradient is shown in Fig. 4. This figure includes also a straight line $\Delta H = \nabla H h$, where $h$ is the height of the chamber.

The jump at $H_c$ (and at $H_{c'}$ in the reverse scanning case) was observed for most of the signals. However, particularly at low pressures, it split into several smaller jumps. Then, if the shape of the jump was not affected, we found that $H_a - H_c$ and $H_a - H_c$ also varied linearly with the field gradient.

### 3. FORMATION OF A HOMOGENEOUS PRECESSING DOMAIN

This strange behavior of the absorption and dispersion signals is in good agreement with the hypothesis of formation of a homogeneously precessing domain (HPD) observed earlier by us in pulsed NMR experiments. Let us consider the spin supercurrent which appears as a result of excitation of NMR in $^3$He-$B$ subjected to an inhomogeneous magnetic field. Let us assume specifically that the cell is a cylinder with axis oriented along the field. Let us also postulate that the field gradient is homogeneous and directed downward (along the $z$ axis), so that the field is minimal at the upper edge of the cell ($z = 0$). If the sample is now subjected to a homogeneous rf field (perpendicular to the $z$ axis) and the frequency of this field is $\omega_{rf}$, the NMR signal is first excited only in a thin layer of $^3$He-$B$ characterized by the

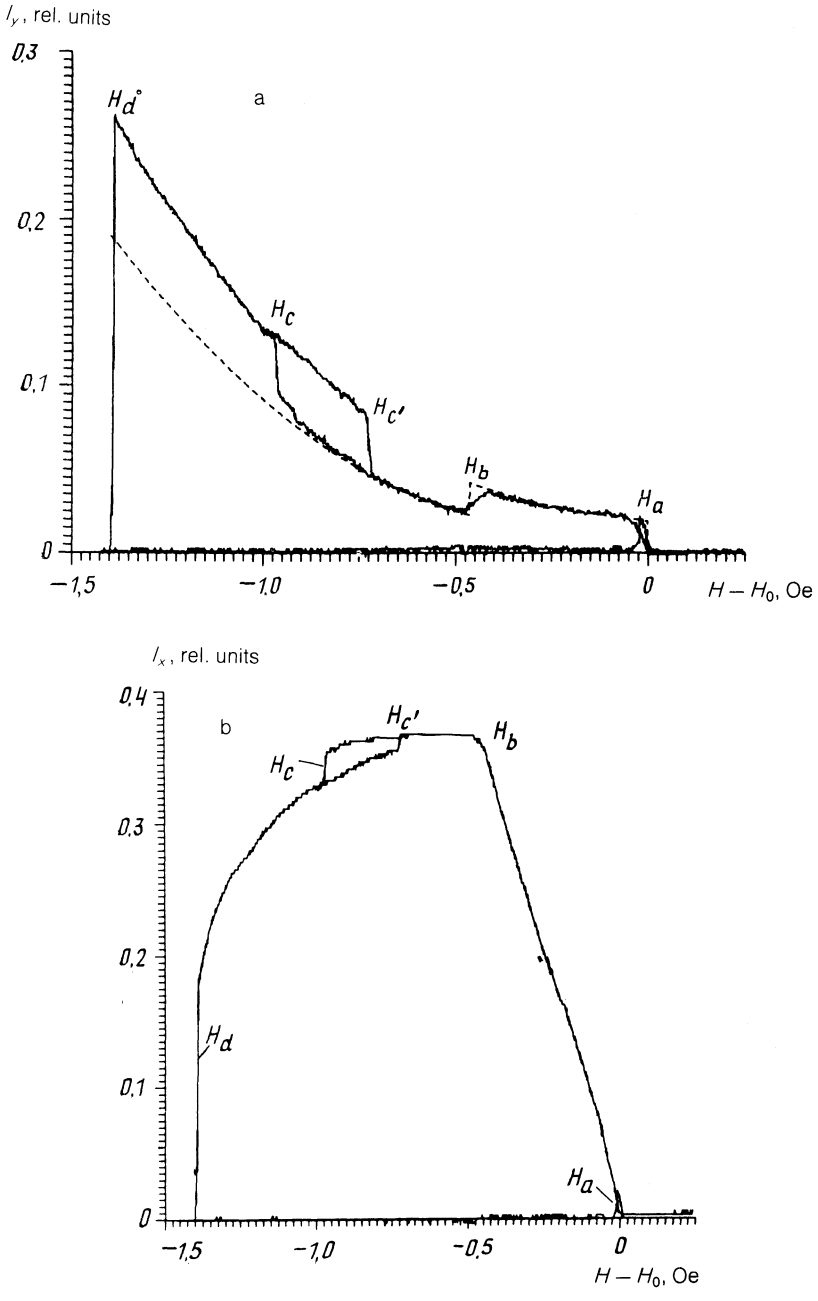


FIG. 2. Typical absorption (a) and dispersion (b) signals observed for $^3$He-$B$ in the presence of a homogeneously precessing domain; $T = 0.57T_c$, $P = 11$ bar.

coordinate $z = z_0$ such that $\omega_{rf} = \gamma H(z_0)$. In this layer the absorption of the rf power is maximal. The resonance condition is not obeyed in a layer above $z$. Consequently, the precession lags in phase here behind the precession in the layer with $z = z_0$. On the other hand, in layers below $z_0$ the precession leads in phase the precession in the layer with $z = z_0$.

The resultant phase gradient can create a spin supercurrent $J_{m_z}$ [see Eq. (9)]. This current transfers the longitudinal magnetization from the upper to the lower layers and increases the angle of tilt of the magnetization from the equilibrium position in the upper layers and reduces it in the lower layers. As long as the rf field amplitude is not too high, the spin current simply creates an asymmetry of the distribution of $\beta = \beta(z)$ (see the Appendix 2). However, if the rf field amplitude is sufficient for the angle $\beta$ to exceed 104°, a completely different behavior is observed. We are now dealing with the dependence of the NMR frequency on the angle $\beta$. In the layers subjected to a weaker magnetic field we can expect such an accumulation of the tilt of the magnetization due to the flow of the spin current that its tilt angle exceeds 104°. The resultant frequency shift compensates for the difference between the magnetic fields $H(z_0) - H(z)$, so that in each layer the precession frequency is in resonance.

Since the transient process resulting in the formation of an HPD is very difficult to describe, the readers interested in this process are referred to the Appendix 1. Here, we shall consider the spatial distribution of the magnetization in an equilibrium situation when an HPD is already formed. This distribution is illustrated in Fig. 5. We can see thus that a state is possible in which the magnetization of $^3$He-$B$ in the layers $z > z_0$ precesses in phase at the rf field frequency. The dynamic NMR frequency shift compensates then for the inhomogeneity of the external magnetic field. The correspond-

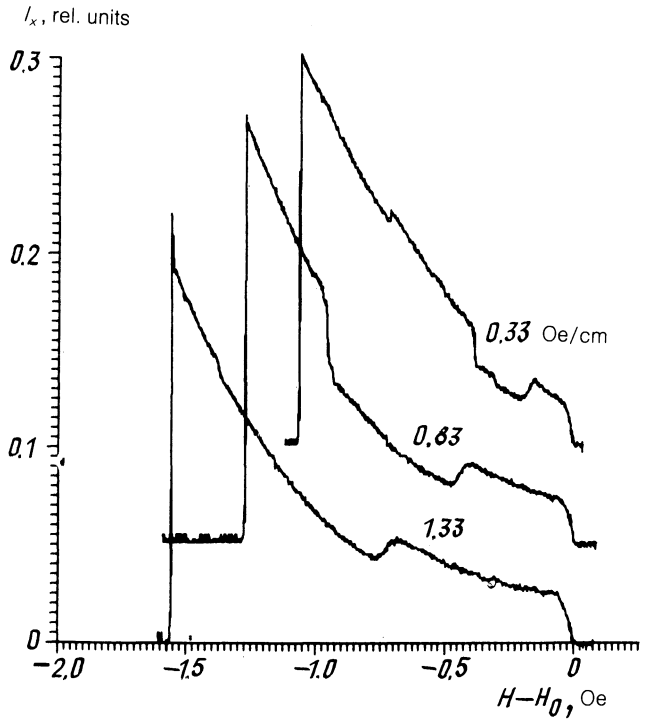


FIG. 3. Absorption signal plotted as a function of the magnetic field gradient.

ing spatial distribution of the angle $\beta$ is very stable, since perturbation of this distribution results in a spatial inhomogeneity of the precession phase, which in turn (via the inhomogeneity of the phase of the order parameter) gives rise to a spin current directed in such a way that this distribution of the angle $\beta$ is restored.

The spin current is zero in the equilibrium distribution case. Below $z_0$ the angle $\beta$ vanishes and the magnetization

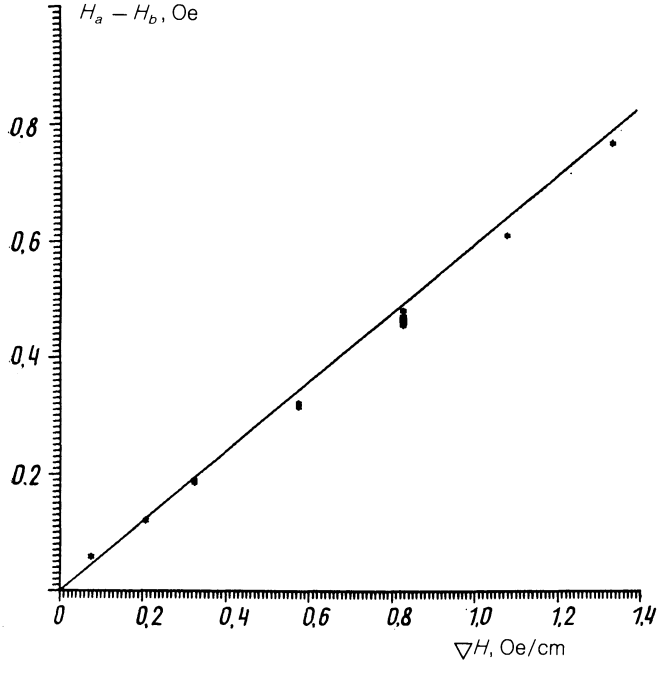


FIG. 4. Dependence of the difference between the characteristic fields $H_a$ and $H_b$ on the magnetic field gradient.

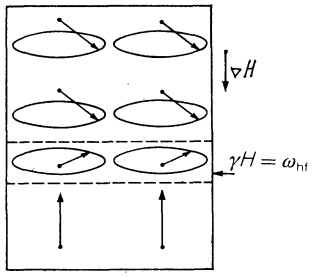


FIG. 5. Spatial distribution of the magnetization in a cell in the presence of a homogeneously precessing domain.

does not precess. In the range of $z = z_0$ there is a domain wall at which $\beta$ changes from 104° to 0°. In spite of the gradient of the angle $\beta$, there is no spin current across this wall, because the term with $\nabla\beta$ is compensated for by the term with $\nabla\alpha$ [see Eq. (9)]. The shape of a domain wall in the absence of an rf field is calculated in Ref. 6. According to a numerical solution of the relevant equations (see both Appendices), the rf field does not change significantly the domain wall shape. In our experiments the domain wall thickness was of the order of 0.1 mm.

If we ignore the dissipation processes, we find that the phase of precession of the HPD should be equal to the phase of the rf field. Then, $M_y$ and consequently the absorption signal should vanish. This value of the HPD phase is very stable. In fact, if the HPD phase lags slightly behind the rf field phase, the HPD begins to absorb energy from the rf field. Consequently, the angle $\beta$ begins to rise and this increases the precession frequency and restores the equality of the rf field and HPD phases. A similar process occurs when the HPD phase leads the rf field phase.

Under real experimental conditions there are always some processes that dissipate the Zeeman energy. In an equilibrium situation the rf field compensates for the loss of energy by the HPD. This creates a difference between the rf field and HPD phases, a component $M_y$ appears, and an absorption signal equal to the energy dissipated by the domain is observed. According to our theory, the value of $M_\perp$ is approximately proportional to the HPD dimensions:

$$M_\perp = \int_{z_0}^{0} dz\, mS \sin\beta,$$

where $S$ is the domain-wall area. On the other hand, we have $M_\perp = (M_x^2 + M_y^2)^{1/2}$ and, consequently, it is proportional to $I_\perp = (I_x^2 + I_y^2)^{1/2}$. When the magnetic field is scanned, the position of $z_0$ changes (linearly in the case of a linear gradient). There should be a corresponding linear rise of the signal $I_\perp$ until $z_0$ shifts outside the chamber. Then, $I_\perp$ should be constant as long as the HPD exists. On reduction of the field the angle $\beta$ should increase to ensure the resonance of the HPD. This increases the energy dissipation due to the Leggett–Takagi relaxation mechanism and, consequently, there should be a change in the phase of precession of the HPD relative to the rf field so as to ensure quality of the energy dissipated in the HPD and that absorbed from the rf field.

The field dependence of $I_\perp$ and of its phase (relative to that of the rf field) is plotted in Fig. 6 for the curves shown in

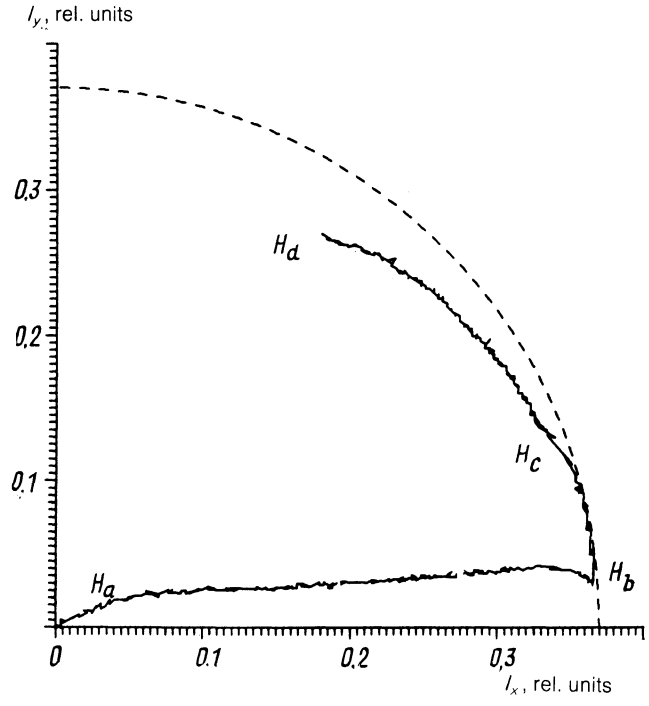


FIG. 6. Hodograph of a cw NMR signal in the presence of a homogeneously precessing domain plotted using the coordinates representing the absorption ($I_y$) and the dispersion ($I_x$); $T = 0.57T_c$; the dashed curve corresponds to the dependence $I_\perp = \text{const}$.

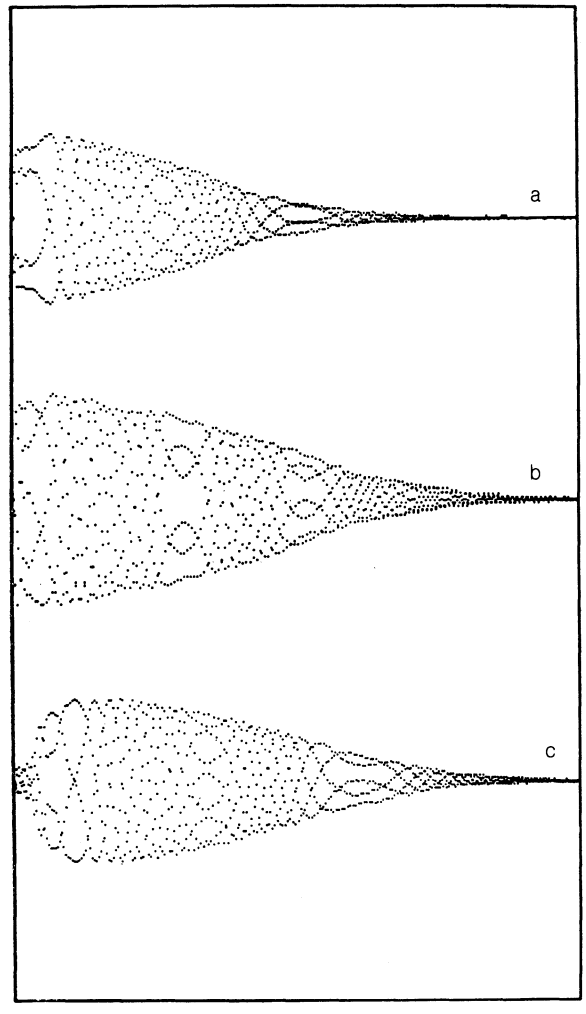


FIG. 7. Digital oscilloscope records of the decay of the free induction signal in $^3$He-$B$ after an rf pulse (c) and after switching off a cw rf field (a,b).

Fig. 2; the abscissa in Fig. 6 represents the dispersion signal $I_x$ and the ordinate is the absorption signal $I_y$. Similar curves were obtained in phase detection of the NMR signal by quadratures. The length of the vector connecting the experimental points to the origin of the coordinate system is $I_\perp$ and the angle between this vector and the abscissa is equal to the difference between the phases of the rf field and $I_\perp$. In the range $H_a$–$H_b$ the signal $I_\perp$ rises linearly, whereas in lower fields it remains approximately constant. We can see that the phase of precession of the HPD lags behind the rf field phase.

Figure 6 shows also that an HPD becomes detached when it tilts away from the rf field by an angle considerably less than 90°. This may be due to a spatial inhomogeneity of the relaxation processes inside the HPD and a consequent spatial twisting of $M_\perp$. The domain should collapse at the moment when the phase $M_\perp$ reaches 90° somewhere in the chamber. The spatial twisting of $M_\perp$ is supported also by the decrease of $I_\perp$ when the field approaches $H_d$. An increase in the amplitude of the rf field in the range $H_a$–$H_b$ decreases $I_y$ in inverse proportion to the field, since the energy dissipated in the domain is independent of the rf field amplitude. The magnitude of $I_\perp$ is independent of the rf field frequency.

The following experiment was carried out to demonstrate that the observed behavior of the NMR signal was indeed associated with the formation of an HPD. After formation of an HPD the pump field was switched off and at the same moment a digital recorder began to measure the signal. When the rf field was switched off, we would expect the HPD to continue to precess creating in the receiving-transmitting coil a signal representing decay of free induction, as found already in pulsed NMR experiments. In the present experiment was used various components of the pulsed NMR spectrometer described in Ref. 5. The signal obtained in this way was similar to a free induction decay signal obtained after excitation of an HPD by a high-power rf pulse. This is illustrated in Fig. 7. The oscillograms $a$ and $b$ were obtained after switching off the rf field, and the oscillogram $c$ was obtained on excitation of an HPD by an rf pulse under the same conditions. The oscillograms $a$ and $b$ differed in respect of the field at which the pumping was switched off. We recorded the oscillogram $a$ in a field $H_a + \frac{2}{3}(H_a - H_b)$, i.e., in the field in which the cell was two-thirds filled with the HPD; the oscillogram $b$ was recorded in a field $H_b$, i.e., when the chamber was completely filled, so that the record $b$ exhibited a considerably greater intensity and duration.

The rf field necessary for the formation of an HPD depended strongly on the position of $z_0$. When $z_0$ was close to the upper cover of the cell, the initial volume in which the magnetization had to be tilted by 104° was small and, consequently, a relatively weak rf field was sufficient for the formation of an HPD. In the case when $z_0$ was at the center of the chamber, the spin current should transfer the magnetization over a greater distance in order to form an HPD. At this moment relaxation appeared (by diffusion and via the Leggett–Takagi mechanism, since the transfer of the transverse magnetization in a magnetic field gradient can be regarded

as an effective frequency shift), leading to the loss of the Zeeman energy and complicating the formation of an HPD. Therefore, an HPD appeared with difficulty when the field was increased, but quite readily when it was reduced.

An HPD could exist, once formed, in an rf field weaker than the field necessary for its formation, because an increase in the dimensions of the HPD hardly affected the dissipation which was determined by the domain-wall area in the case of a small domain, whereas the fraction of the volume of $^3$He-$B$ capable of absorbing the rf field energy increased.

We do not know the origin of the jump at the point $H_c$ and can only propose the following model. When an HPD penetrated into the channel, it filled the region where there was no rf field. Relaxation occurring in this region was compensated by a spin supercurrent flowing from the bulk of the HPD. At some point the spin current could exceed the critical value creating a phase-slip center.[11] This resulted in additional losses. Consequently, the HPD in the channel was destroyed and the absorbed power increased because of the spin current that transferred the energy to the channel.

We shall conclude by noting that the application of a field slightly higher than $H_b$ resulted in oscillations of the absorbed power at a frequency 50–100 Hz. These oscillations were clearly due to spontaneous vibrations of the domain wall because of its interaction with the walls of the cell. Low frequency ($\sim 10$ Hz) oscillations of the absorbed power were also observed in fields $H_d < H < H_c$ at a pressure of 0.6 bar. The nature of these oscillations was not clear. It should be pointed out that several vibration modes could be exhibited by an HPD.[12] Two modes of such vibrations, torsional vibrations of an HPD and surface waves on a domain wall, were revealed by pulsed experiments.[13,14] A study of vibrations of an HPD under cw NMR conditions will be an interesting task for the future.

## 4. PROCESSES OF MAGNETIC RELAXATION OF A HOMOGENEOUSLY PRECESSING DOMAIN

The power absorbed by an HPD from the rf field is equal to the power dissipated in the domain. We shall now consider qualitatively the behavior of the absorption signal as a function of the magnetic field. Relaxation of the Zeeman energy in an HPD is due to, firstly, diffusion relaxation of the domain wall. This mechanism of magnetic relaxation had been investigated theoretically[7] and observed experimentally in the formation of an HPD under pulsed NMR conditions.[5] Secondly, we have the familiar relaxation mechanisms suggested by Leggett and Takagi.[15] This relaxation mechanism appears in $^3$He-$B$ when the precession frequency differs from the Larmor value and, finally, when a surface relaxation mechanism proposed in Ref. 16 can exist, because this mechanism results in dissipation of the Zeeman energy on the walls of a cell oriented at right-angles to a magnetic field. The absorption due to spin diffusion across a domain wall is independent of the domain size and is proportional to the domain wall area. This surface relaxation process increases linearly on increase of the domain length. In a field $H_b$ the domain fills the whole cell, the domain wall enters the channel containing the cell to the heat exchanger, and its area decreases strongly. The diffusion relaxation disappears practically completely, but the surface relaxation is not affected and the subsequent rise of the absorption is due to the Leggett–Takagi mechanism. The maximum value of the power which an HPD can absorb from an rf field is governed by the rf field amplitude in accordance with $\dot{W} = \omega M_\perp H_1$. As the power dissipated in the HPD approaches this value, the domain is destroyed (field $H_d$).

We shall describe the absorption signal quantitatively by writing down the energy dissipated in a domain and on its wall[5,7,15,16]:

$$\dot{W} = \chi H^2 \left[ \omega_{rf}^{1/3} \frac{D\sigma(\nabla\omega)^{1/3}}{c_s^{2/3}} S + \frac{15}{16} \tau_{LT} (\nabla\omega)^2 \int_0^{z_0} (z - z_0)^2 \, dV \right] + 2\dot{W}_s \pi R |z_0|. \quad (11)$$

In this equation the first term represents the magnetic relaxation process on a domain wall because of spin diffusion, the second term corresponds to the Leggett–Takagi relaxation mechanism, whereas the third term represents the surface relaxation process; $\omega_{rf}$ is the precession frequency equal to the rf field frequency; $D$ is the spin diffusion coefficient; $c_s$ is the velocity of spin waves; $\nabla\omega = -\gamma\nabla H$; $\tau_{LT}$ is the characteristic Leggett–Takagi relaxation time; $z_0$ is the length of the investigated domain, which is $z_0 = (H_a - H)/\nabla H$ in the range $H_a > H > H_b$, and $z_0 = L$ is the length of the cell when $H < H_b$; $\sigma$ is a number representing the shape of the domain wall and is close to 1.1; $S$ is the domain wall area (which changes when the wall travels from the cell to the capillary); $R$ is the radius of the cell; $W_s$ is a coefficient representing the surface relaxation rate.

The dashed curve in Fig. 2a is the dependence obtained by approximating the experimental curve in accordance with Eq. (11). It should be pointed out that the term which is a cubic function of the HPD dimensions (corresponding to the Leggett–Takagi relaxation) is determined mainly in the range of fields $H_b$–$H_d$ and this can be done to a high degree of accuracy. The term independent of the domain size (and corresponding to the diffusion relaxation process) is found mainly from the size of the jumps in the fields $H_a$ and $H_b$, and again this can be done quite accurately. The dependences of these terms on the magnetic field gradient are in agreement with the diffusion and Leggett–Takagi relaxation mechanism.

The relaxation mechanism proposed in Ref. 16 was checked by Anita de Waard who made an additional cell in which the side surface was increased threefold by eleven Mylar ribs. To our surprise, we found that the term depending linearly on the domain size was independent of the dimensions of the lateral surface. On the other hand, a numerical calculation of the operation of the detector part of the spectrometer demonstrated that the absorption signal could include corrections because of a strong dispersion, which resulted in the appearance of a term quadratic in respect of the domain size. The fitting of the experimental data allowing for thes corrections had practically no effect on terms cubic and zeroth in respect of the domain size, but it did not allow us to distinguish clearly the linear term from the quadratic one.

For a quantitative determination of the relaxation processes we calibrated the detector part of the spectrometer. The power dissipated in the domain was assumed to be (in the Gaussian system of units)

$$\dot{W} = U_y U_0 c^2 / 2aQ\omega L, \quad (12)$$

where $U_y$ and $U_0$ are the amplitudes of the voltage representing the rf absorption and pump signals; $a$ is the spectrometer gain; $L$ is the inductance of the detector coil; $Q$ is the $Q$ factor of the resonating circuit; $c$ is the velocity of light in vacuum. We compared this expression with Eq. (11) and obtained, under the experimental conditions of Fig. 2, a value $\tau_{LT} = 2.3\times10^{-7}$ s and a coefficient $D\sigma/c_s^{2/3} = 1.84\times10^{-3}$ $(\text{cm}^4/\text{s})^{1/3}$ representing the process of spin diffusion across the domain wall. The value of $\tau_{LT}$ was found by this method to a high degree of precision (set by the precision of the spectrometer calibration) and agreed with the results of earlier measurements.[17] In the spin diffusion measurements it was necessary to calculate the coefficient $\sigma$, which was a function of the domain wall shape. In the case of pulsed NMR it was found that $\sigma = 1.1$ and for a continuous NMR the same coefficient could depend on the rf field amplitude.

We were thus left with one other term in the absorption signal, which could be linear or quadratic in the domain size. Under the experimental conditions described above when the cell was filled completely, this term was responsible for loss of energy at the rate of $\sim$0.1 nW. In a cell with Mylar ribs it amounted to 0.12 nW. If we assume that the surface relaxation process was responsible for this distance in the dissipated energy, then in the case of $W_S$ we obtained a value of the order of 0.01 nW/cm$^2$, which was close to the estimates given in Ref. 16 ($\approx$0.02 nW/cm$^2$ under our experimental conditions). We assumed that the remainign signal ($\approx$0.09 nW) was not due to absorption, but due to a shift of the resonance frequency of the circuit because of the large dispersion signal (represented by the term quadratic in respect of the domain size).

We therefore concluded that our method was suitable for investigation of the Leggett–Takagi and diffusion mechanisms. The surface relaxation mechanism proposed in Ref. 16 would require a further improvement in this method.

## 5. CONCLUSIONS

We demonstrated that a homogeneously precessing domain (HPD) can be formed under cw NMR conditions and can be maintained indefinitely. This extends greatly the capabilities of experimental studies of spin supercurrents and magnetic relaxation processes in $^3$He-$B$. In particular, we were able to observe the flow of a spin supercurrent in a narrow channel containing two independent HPDs, and also the associated phase-slip regime,[18] as well as a regime analogous to the Josephson effect in thin superconducting wires.[19] Interesting results were also obtained on spatial rotation of an OPD. The vortices resulting from rotation gave rise to additional magnetic relaxation. In this way an OPD made it possible to investigate the properties of rotating $^3$He.

The authors are deeply grateful to I. A. Fomin for a fruitful cooperation and constant theoretical consultations, to A. de Waard, J. Hecchi, D. A. Sergatskiĭ, and G. K. Tvalashvili for their help in the preparatory stages and in some experiments.

## APPENDIX 1

A clear picture of the processes of formation of a two-domain structure of precessing magnetization of $^3$He-$B$ was obtained by numerical solution of the system of equations (6) allowing for spin diffusion and for an rf field. The calculations were carried out on a computer using the Herr method. As pointed out in Sec. 1, the system of equations (6) describes the behavior of the magnetization of $^3$He-$B$ in the range of angles of tilt of the magnetization from 0 to 104°. An analytic transition across the point $\beta = 104°$ can be tackled by solving a system of equations with an additional variable $\Phi$, which greatly complicates the numerical calculations. However, if we assume that the dipole–dipole interaction is much stronger than the other interactions and that the condition (8) corresponding to the minimum of the dipole–dipole interaction is always satisfied, an additional gradient frequency shift is observed and it becomes infinite in the limit $\beta\to\cos^{-1}(-1/4)$.

A numerical analysis thus shows that formation of an HPD is possible because of compensation of the Larmor frequency gradient by a frequency shift gradient. Since in a numerical analysis we were interested in the behavior of the magnetization in the range $0<\beta<104°$, we limited the solution of the system (6) bearing in mind that it was quantitatively wrong in the vicinity of $\beta\approx104°$. However, in the qualitative sense this solution differs little from that expected for real $^3$He-$B$, when the frequency shift is known to be of the dipole–dipole origin and appeared in the range $\beta>104°$. Figure 8 shows the change in the spatial distributions of the longitudinal magnetization ($\cos\beta$) as a function of time in the pulsed NMR (a) and in the presence of an rf field (b); these results were obtained by numerical solution of the system of equations (6). We allowed for the processes of magnetic relaxation due to spin diffusion of the normal component of $^3$He-$B$ by introducing on the right-hand side of the system (6) the following terms:

$$D[u''+(\nabla\alpha)^2\sin^2\beta+(\nabla\beta)^2], \tag{6'}$$

$$D\left\{\left[\left(\frac{3}{1+4u}\right)^{1/2}\frac{1}{1+u}(\nabla\alpha)^2\sin^2\beta+(\nabla\beta)^2\right]\right.$$

$$\left.+\alpha''+\nabla\alpha\nabla\beta\,2\,\text{ctg}\,\beta\right\}.$$

In both cases the calculations were carried out for $c_\parallel = 800$ cm/s assuming that the spin diffusion coefficient was $D = 0.1$ cm/s$^2$ and that the field gradient was $\nabla H = 0.2$ Oe/cm. The absence of a spin current was taken to be the boundary condition for the walls of a cell of length 2.5 mm. The behavior of the magnetization after an initial deflection by an angle 90° ($\cos\beta = 0$) is shown in Fig. 8a. We can clearly see the transient process creating a two-domain structure. Moreover, the results demonstrate that oscillations are associated with a change in the domain wall thickness.

In numerical modeling of the processes occurring in the case of cw NMR we considered the formation of a two-domain structure after application of an rf field of constant intensity (Fig. 8b). In this case it was assumed that initially the magnetization was not tilted from the equilibrium orientation. We assumed the application of an rf field of frequency equal to the Larmor frequency of spins in the region identified by an arrow. The amplitude of the rf field was $5\times10^{-3}$ Oe. The results show clearly a transient process during which an equilibrium is established between the phase of the rf field and the phase of the magnetization precession, and the power absorbed by a domain from an rf field is equal to the dissipated power.

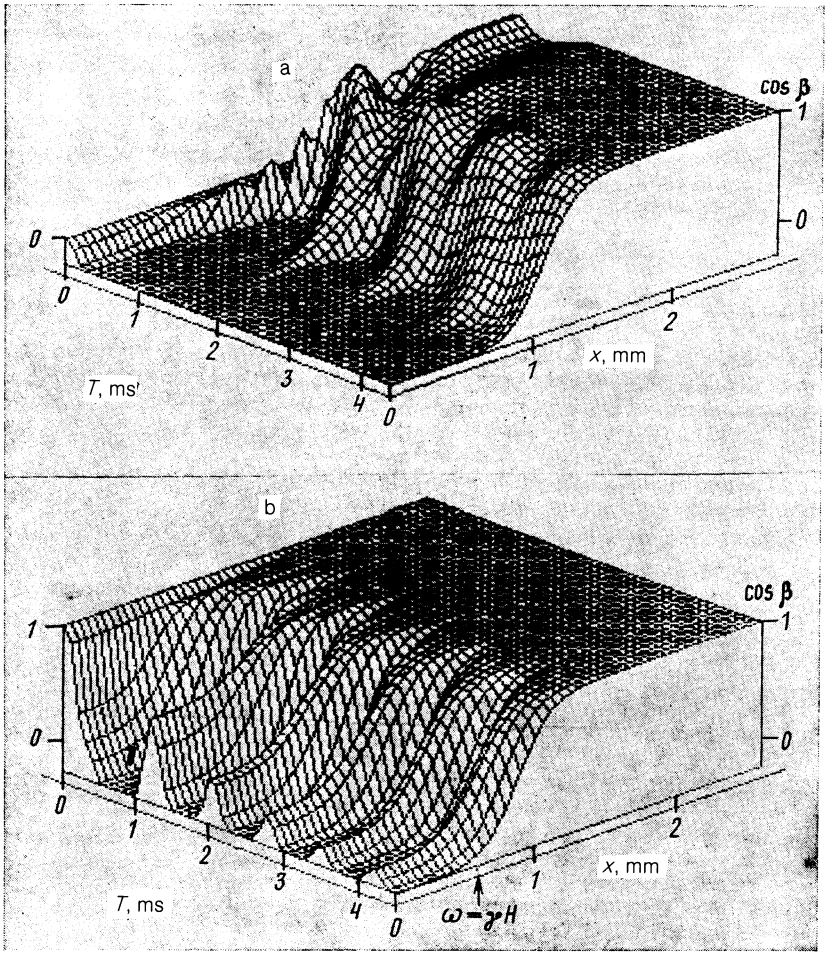


FIG. 8. Time dependences of the spatial distribution of the longitudinal magnetization ($\cos\beta$) after an rf field pulse (a) and after switching on of a continuous rf field (b).

## APPENDIX 2

The presence of superfluid spin currents alters the behavior of the magnetization of $^3$He-$B$ in the presence of a weak rf field before formation of an HPD domain. The influence of such currents on the distribution of the precessing magnetization was studied by solving the system of equations (6) and (6′) in the presence of an rf field of constant amplitude $\approx 10^{-3}$ Oe in a sample subjected to a gradient of a static magnetic field. By way of illustration, Fig. 9 shows the spatial distribution of a transverse magnetization component directed at right-angles to the rf field $M_y$. This figure shows the distribution obtained both in the absence of a spin current (dashed curve) and in its presence (continuous curve). The solutions were obtained for $\nabla H = 0.2$ Oe/cm, $D = 0.075$ cm/s$^2$, and $c_{\|} = 800$ cm/s. It is clear from the dashed curve that the process of spin diffusion results in a transfer of the magnetization from the resonant region, which reduces the value of $M_y$ at the center of the line and increases it symmetrically in the wings. If we bear in mind also the superfluid spin current, we find that the distribution of $M_y$ becomes asymmetric. In the direction of a weaker magnetic field, it has the form of a damped wave. The spatial distribution of the other component of the transverse magnetization ($M_x$) in fields $H < |\omega/\gamma|$ is of the same form, but it is shifted in phase by 90°. Therefore, a superfluid spin current results in a tilt of the magnetization well away from a resonance and the tilt is in the direction of a weaker magnetic field. This results in twisting of $M_{\perp}$ into the shape of a three-dimensional helix.

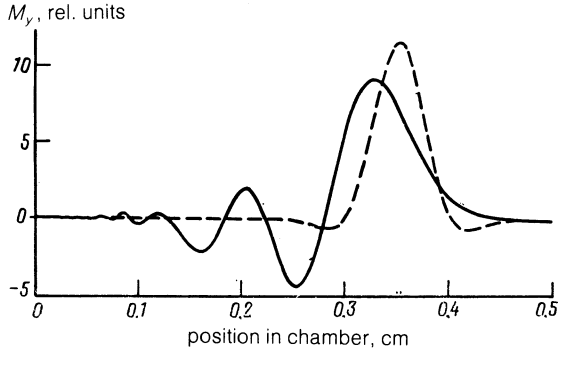


FIG. 9. Distribution of the component $M_y$ of the transverse magnetization of $^3$He-$B$ in a chamber subjected to a magnetic field gradient and a weak rf field. The dashed curve represents the distribution of $M_y$ obtained allowing for the spin diffusion process and the continuous curve allows also for the superfluid spin current.

This solution was obtained for an infinite cell. If the cell wall is located at a distance of the order of the magnetization transport length, the system of equations (6) must be solved subject to a suitable boundary condition. This gives rise to solutions of the form which, like the absorption of the rf energy, depends on what part of the solution corresponds to the wall. The change in the wall position gives rise to oscillations of the NMR signal associated with modification of the solutions when the number of turns of the helix changes. Such oscillations were observed experimentally by scanning

the magnetic field. On the other hand, the same oscillations could be regarded as modes of standing spin waves.

[1)]Lebedev Physics Institute, Academy of Sciences of the USSR, Moscow.
[2)]Physics Department, Moscow State University.

[1]D. D. Osheroff, in: *Quantum Fluids and Solids* (Proc. Second Intern. Symposium, Sanibel Island, FL, 1977, ed. by S. B. Trickey, E. D. Adams, and J. W. Dufty), Plenum Press, New York (1977), p. 161.
[2]R. A. Webb, Phys. Rev. Lett. **39**, 1008 (1977).
[3]W. F. Brinkman and H. Smith, Phys. Lett. A **53**, 43 (1975).
[4]A. S. Borovik-Romanov, Yu. M. Bun'kov, V. V. Dmitriev, and Yu. M. Mukharskiĭ, Pis'ma Zh. Eksp. Teor. Fiz. **40**, 256 (1984) [JETP Lett. **40**, 1033 (1984)].
[5]A. S. Borovik-Romanov, Yu. M. Bun'kov, V. V. Dmitriev, *et al.*, Zh. Eksp. Teor. Fiz. **88**, 2025 (1985) [Sov. Phys. JETP **61**, 1199 (1985)].
[6]I. A. Fomin, Pis'ma Zh. Eksp. Teor. Fiz. **40**, 260 (1984) [JETP Lett. **40**, 1037 (1984)].
[7]I. A. Fomin, Zh. Eksp. Teor. Fiz. **88**, 2039 (1985) [Sov. Phys. JETP **61**, 1207 (1985)].
[8]D. M. Lee and R. C. Richardson, in: *The Physics of Liquid and Solid Helium* (ed. by K. H. Benneman and J. B. Ketterson), Part 2, Wiley, New York (1978), p. 289.
[9]I. A. Fomin, Zh. Eksp. Teor. Fiz. **93**, 2002 (1987) [Sov. Phys. JETP **66**, 1142 (1987)].
[10]A. S. Borovik-Romanov, Yu. M. Bun'kov, V. V. Dmitriev, *et al.*, Prib. Tekh. Eksp. No. 3, 185 (1985).
[11]Yu. M. Bun'kov, V. V. Dmitriev, Yu. M. Mukharskiĭ, and G. K. Tvalashvili, Zh. Eksp. Teor. Fiz. **94**(2), 154 (1988) [Sov. Phys. JETP **67**, 300 (1988)].
[12]I. A. Fomin, Pis'ma Zh. Eksp. Teor. Fiz. **43**, 134 (1986) [JETP Lett. **43**, 171 (1986)]
[13]Yu. M. Bun'kov, V. V. Dmitriev, and Yu. M. Mukharskiĭ, Pis'ma Zh. Eksp. Teor. Fiz. **43**, 131 (1986) [JETP Lett. **43**, 168 (1986)].
[14]Yu. M. Bunkov, Proc. Eighteenth Intern. Conf. on Low Temperature Physics, Kyoto, 1987, in: Jpn. J. Appl. Phys. **26**, Suppl. 26-3, 1809 (1987).
[15]A. J. Leggett and S. Takagi, Phys. Rev. Lett. **34**, 1424 (1975).
[16]T. Ohmi, M. Tsubota, and T. Tsuneto, Proc. Eighteenth Intern. Conf. on Low Temperature Physics, Kyoto, 1987, in: Jpn. J. Appl. Phys. **26**, Suppl. 26-3, 169 (1987).
[17]G. Eska, K. Neumaier, W. Schoepe, *et al.*, Phys. Lett. A **87**, 311 (1982).
[18]A. S. Borovik-Romanov, Yu. M. Bun'kov, V. V. Dmitriev, and Yu. M. Mukharskiĭ, Pis'ma Zh. Eksp. Teor. Fiz. **45**, 98 (1987) [JETP Lett. **45**, 124 (1987)].
[19]A. S. Borovik-Romanov, Yu. M. Bun'kov, A. de Waard, *et al.*, Pis'ma Zh. Eksp. Teor. Fiz. **47**, 400 (1988) [JETP Lett. **47**, 478 (1988)].
[20]D. Candela, N. Masuhara, D. S. Sherrill, and D. O. Edwards, J. Low Temp. Phys. **63**, 369 (1986).

Translated by A. Tybulewicz